

# PERFORMANCE OF THREE ALTERNATIVE SURFACING PROCESSES ON BLACK SPRUCE WOOD AND THEIR EFFECTS ON WATER-BASED COATING ADHESION

*Julie Cool*

PhD Candidate

E-mail: julie.cool@fpinnovations.ca

*Roger E. Hernández\*†*

Professor

Centre de Recherche sur le Bois

Département des Sciences du Bois et de la Forêt

Pavillon Gene-H. Kruger

2425, rue de la Terrasse

Université Laval

Québec (Québec) Canada G1V 0A6

E-mail: roger.hernandez@sbf.ulaval.ca

(Received February 2011)

**Abstract.** Surface quality and water-based coating performance of samples prepared by oblique cutting, helical planing, and face milling were studied. Oblique cutting and helical planing generated surfaces with similar features. Samples had little subsurface damage and fibrillation, and few cell lumens were accessible on the surface to favor coating penetration. As a result, these samples had lower surface roughness and wetting properties than face-milled ones. Face-milled samples were defined by more subsurface damage, fibrillation, and open lumens that favored coating penetration. However, the pull-off strength of face-milled samples was significantly lower after accelerated weathering than the oblique-cut or helical-planed samples. Hence, oblique cutting and helical planing are suitable for preparing surfaces of black spruce prior to coating application. No correlations were detected between surface quality parameters and adhesion, which indicates that pull-off tests have to be determined to quantify coating adhesion on surfaces of this wood species.

**Keywords:** Black spruce wood, oblique cutting, face milling, helical planing, surface quality, coating.

## INTRODUCTION

Sanding is one of the most skill-based, time-consuming, and expensive operations in the wood industry (Taylor et al 1999) besides being a health hazard (d'Errico et al 2009). Because sanding produces defect-free uniform surfaces (Richter et al 1995), it is widely used in the industry prior to coating application. However, the cutting forces involved are generally greater than those in planing processes (Stewart 1980, 1989; Hall and Heard 1982; Stewart and Crist 1982). According to several reports, sanded surfaces are characterized by lumens clogged with

fine dust, scratches, and packets of microfibrils torn out from cell walls (Murmanis et al 1983, 1986; de Moura and Hernández 2006b). Crushing and clogging of cells hinder penetration (de Meijer et al 1998), whereas slight fibrillation and scratches accelerate spreading of liquid coatings on sanded surfaces. Benefits of fibrillation for mechanical adhesion of coating films have been shown for sanded surfaces of sugar maple wood (de Moura and Hernández 2005). Recently, Cool and Hernández (2011a) reported that no significant differences were detected for shear strength of glued black spruce wood samples machined by four different machining processes, including sanding. Hence, finding alternative processes could decrease the use of the sanding, which could

---

\* Corresponding author

† SWST member

lower production costs and increase air quality in facilities.

Oblique cutting differs from orthogonal cutting by an inclination given to the knife edge, called oblique angle ( $i$ ). When  $i$  increases, effective rake angle ( $\alpha$ ) also increases, whereas effective clearance ( $\gamma$ ) and knife ( $\beta$ ) angles decrease (Ozaki and Kimura 1989; Jin and Cai 1996, 1997). Knife edge radius also decreases as oblique angle increases, which enhances tool sharpness (Jin and Cai 1997). For sugar maple wood, an increase in  $i$  induced an increase in surface roughness that was minimized by increasing  $\alpha$  (de Moura and Hernández 2007). Also, smoothness of oblique-cut surfaces and their intact sound tissues could minimize the effect of aging (de Moura et al 2010).

Face milling is generally considered to be the result of the combined action of cutting edges located at the periphery and the face of a cutter to machine a flat surface perpendicular to the cutter axis (Stewart 1974). This process typically occurs across the grain, and suitable levels of fibrillation have been reported for paper birch (Hernández and Cool 2008a, 2008b), sugar maple, and red oak (de Moura et al 2010). Lower-density wood species such as white pine (de Moura et al 2010) and black spruce (Cool and Hernández 2011a) showed greater fibrillation than those observed for hardwoods. This level of fibrillation increases the actual surface available for mechanical anchorage with an adhesive and could contribute to improved adhesion strength.

Knives in helical planing are mounted on the periphery of a cutterhead at an angle to the axis of rotation, which forms a continuous oblique cutting edge (Stewart 1971). Torn grain, raised grain, chip marks, noise levels, and power consumption are decreased as a result of the gradual cutting action of helical planing (Stewart and Hart 1976; Jones 1994). According to Stewart and Lehmann (1974), the surface generated in helical planing is similar to that obtained in conventional peripheral planing. Planing in the 0-90° direc-

tion further improved surface quality (Stewart 1975; Koch 1976) and did not induce subsurface damage in sugar maple (de Moura and Hernández 2006a) or paper birch woods (Hernández and Cool 2008a). However, this feeding direction restricts the planing process to relatively short pieces of wood as their maximum length is limited by the cutterhead length.

This study evaluated effects of three alternative planing processes, oblique cutting, face milling, and helical planing, on the surface quality of black spruce wood for water-based coating. Microscopy, surface roughness, and wettability analyses were used to assess surface quality. Performance of a water-borne coating film was assessed by accelerated aging and pull-off tests.

## MATERIALS AND METHODS

### Testing Materials

Black spruce wood (*Picea mariana* [Mill.] B.S.P.) was selected for this study. Two hundred seventy 1.5-m (L) flat-sawn boards were kiln-dried and stored in a conditioning room at 20°C and 40% RH until they reached 10% equilibrium moisture content (EMC). After conditioning, all sections were machined at 52 mm (T) width and 22 mm (R) thickness. A section 25 mm long was cross-cut from each specimen to measure average ( $455 \text{ kg/m}^3$ ) and standard deviation ( $35 \text{ kg/m}^3$ ) of basic density (oven-dry mass divided by green volume). Specimens were then divided into nine groups with average density of  $455 \text{ kg/m}^3$  each. Subsequently, each group underwent a surfacing treatment. After surfacing, samples were re-sectioned to prepare specimens for roughness (50 mm [L]), microscopy (25.4 mm [L]), wettability (160 mm [L]), and coating application (620 mm [L]). After coating, two matched samples were sawn. One sample underwent accelerated aging treatment before being submitted to the adhesion test and the other one remained untreated.

### Machining Treatments

Three different machining processes were used to surface the specimens. Previous cuts were carried out to level samples prior to each surfacing treatment. Oblique cutting was performed with a Super Meca (Marunaka Tekkosho Inc., Shizuoka, Japan) working at 65 m/min feed speed and 0.02-mm cutting depth. The freshly sharpened high speed steel knife had a 32° nominal knife angle and a 58° nominal rake angle. Oblique angle ( $i$ ) was studied at 10, 35, and 60°, which generated effective rake angles ( $\alpha$ ) of 59, 64, and 74° (Ozaki and Kimura 1989). Face milling was carried out with a Rotoplane 16T (Ogden Enterprises Inc., Matthews, NC) provided with a cutter disk holding new insert carbide knives at an angle of 60°. The positive axial  $\alpha$  and radial  $\alpha$  (Stewart 1974) were 20 and 13°, respectively. Feed speed was studied at 27.3, 36.4, and 27.3 m/min. Thirty-four insert knives were used for the first two feed speeds, which yielded feed per tooth (FT) of 0.26 and 0.34 mm, respectively. Seventeen insert knives were used for the third feed speed, which resulted in a FT of 0.53 mm. Cutting depth was 1 mm. Samples were fed through the center line of the cutter disk and were therefore planed to nearly the 13-90° direction. Helical planing treatments were performed with a Casadei R63H3 (Casadei Macchine, Villa Verucchio, Italy) 0.61-m planer provided with two new flexible knives. The  $\alpha$  and helix angles were 30 and 14°, respectively. Feed speed was studied at 5.7, 7.2, and 9.5 m/min, which corresponded to wavelengths of 1.11, 1.43, and 2.00 mm. Cutting depth was 1 mm.

### Microscopic Evaluation

Cubes of 10 mm were cut to observe tangential and end-grain surfaces. Tangential surfaces were used to evaluate fibrillation level and open lumens, whereas end-grain surfaces were used to analyze cell damage and coating penetration. One end-grain surface was carefully cut with a razor blade mounted on a microtome. All cubes were then desiccated with

phosphorous pentoxide ( $P_2O_5$ ) for 1 week and mounted on standard aluminum stubs with silver paint. Environmental scanning electron microscopy micrographs were taken for two representative machined samples for each machining treatment.

### Surface Topography Measurements

Roughness measurements were carried out on defect-free zones with a Micromeasure confocal microscope (Stil, Aix-en-Provence, France). A surface of 12.5 (L) by 12.5 mm (T) was analyzed per sample. Data were collected with Surface Map 2.4.13 software using an acquisition frequency of 300 Hz and a scanning speed of 12.5 mm/s. 3D roughness parameters were determined with Mountain software. A cut-off length of 2.5 mm combined with a Robust Gaussian filter (ISO 2002) was used for calculations. Arithmetical mean deviation of the profile ( $S_A$ ), root mean square deviation of the profile ( $S_Q$ ), maximum profile peak height ( $S_P$ ), and maximum profile valley depth ( $S_V$ ) were calculated according to ISO (1997). Reduced peak height ( $S_{PK}$ ) and reduced valley depth ( $S_{VK}$ ) were calculated from the Abbot curve according to ISO (1996).

### Wettability Measurements

Wetting properties were evaluated within 8 h after machining treatments. Wetting analyses were performed with an FTÅ D200 imaging goniometer (Folio Instruments Inc., Ontario, Canada) at 20°C. One drop ( $\approx 6 \mu\text{L}$ ) of pure water was added to wood surfaces with an injection microsyringe. A frame grabber recorded changes in droplet profile during the first 120 s of wetting. Measurements were carried out in the longitudinal direction because wetting is more important and constant in the fiber direction (Gardner et al 1991; de Meijer et al 2000). Contact angle was calculated as a mean of both sides of the drop to compensate for any horizontal variations. Wetting rate was calculated as  $\Delta\theta/\Delta t$  to assess spreading and penetration of pure water during the first 30 s of wetting.

For surface energy measurements, initial contact angle of formamide was measured. Non-polar and polar components of surface energy were calculated using the harmonic mean method (Wu 1971). A recent literature review claims that, to date, no procedure has been developed for determining absolute values of surface energy (Piao et al 2010). However, several researchers have used this method to describe physicochemical changes of wood surfaces produced by different treatments (Wang et al 2007; Wolkenhauer et al 2007).

### Coating Application Procedure

Machined surfaces were coated within 8 h after machining treatments. Prior to coating, samples were placed face against face to keep contamination at minimum levels. Two coats of an acrylic water-based coating, Laurentide-Innocryl PF, was air-sprayed (150  $\mu\text{m}$ ) at room temperature according to the manufacturer's specifications. The coating was then cured in an IR oven following methodology established with the coating manufacturer.

### Accelerated Aging

One set of specimens underwent accelerated aging treatments in a Cincinnati SubZero (Cincinnati, OH) environmental stimulation chamber (WM-906-MP2H-3-SC/WC) with temperature and RH precisions of  $\pm 1^\circ\text{C}$  and  $\pm 3\%$ , respectively. Treatment was based on ASTM (1998) and consisted of four cycles of 48 h at  $50^\circ\text{C}$  and 10% RH followed by 48 h at  $50^\circ\text{C}$  and 90% RH. Prior to treatment, specimen ends were sealed with paraffin to decrease moisture exchange through the cross-section. After aging, specimens were conditioned at  $20^\circ\text{C}$  and 40% RH until they reached their initial EMC (10%).

### Adhesion Tests

Adhesion of aged and unaged films was evaluated by means of a pull-off test according to ASTM (2002). A MTS QT5 universal testing machine (MTS, Eden Prairie, MN) with a

maximum load capacity of 5 kN and  $\pm 0.12\%$  precision was used. Small 20-mm-diameter dollies were glued on the film surface with Araldite (Huntsman International, LLC, Salt Lake City, UT) 2011 two-part epoxy resin. After 24 h of curing at  $20^\circ\text{C}$  and 40% RH, perimeters of the glued dollies were carefully incised to prevent propagation of failures out of the tested area. Pulling was applied at 1 mm/min until separation of the dolly from the substrate. Maximum normal pull strength at rupture was recorded.

### Statistical Analyses

The data followed a randomized block design, and results from mechanical tests were analyzed with the mixed procedure in SAS as repeated measures. Surface topography, wettability, and surface energy were analyzed as a one-way analysis of variance following the glm procedure. Mean difference comparison tests were performed at the 5% probability level when required. Simple correlations between surface quality parameters and pull-off results were studied using the corr procedure. Analysis was performed with the SAS statistical package, version 9.2 (SAS 2007).

## RESULTS AND DISCUSSION

### Microscopy

**End-grain surfaces.** Oblique-cut samples prepared with oblique angles of 10 and  $35^\circ$  were virtually free of surface defects (Fig 1a–b). The use of both oblique angles did not appear to be sensitive to the density gradient between earlywood and latewood. This agrees with previous results obtained by de Moura et al (2010) and Cool and Hernández (2011a). However, increasing the oblique angle up to  $60^\circ$  induced microruptures in latewood cells (arrows in Fig 1c). This contrasts with what was observed for earlywood cells (Fig 1d). As oblique angle increased, the lateral component of the cutting force increased (de Moura and Hernández 2007). de Moura and Hernández (2007) also

reported that higher oblique angles produced more surface defects, although a pressure bar was used. The occurrence of surface defects could be more important for black spruce wood because of its number of small knots. Thus, the combination of the lateral force with grain deviation could result in additional microruptures. The level of coating penetration is also shown in Fig 1. Apparently, the coating was mainly deposited on the surface and only penetrated the first layer of cells. Similar observations were reported when gluing oblique-cut samples of black spruce wood (Cool and Hernández 2011a). As the oblique angle reached 60°, the coating filled more cells in the first layer (Fig 1c–d). The higher number of

microruptures observed in these samples favored coating penetration in the samples.

Compared with oblique cutting, face milling produced greater surface damage (Figs 1 and 2). As subsequently explained, the rake angle used in the experiment was probably not the optimum to obtain good results. For the three studied cutting conditions, surfaces were characterized by subsurface damage in the form of cell crushing, deformation, and microruptures. At 0.53-mm FT, permanent deformation up to the first two rows of earlywood cells ( $\approx 70 \mu\text{m}$ ) was observed (Fig 2a). Microruptures through cell walls were also seen in these samples. In latewood cells, the top layer of cells was crushed

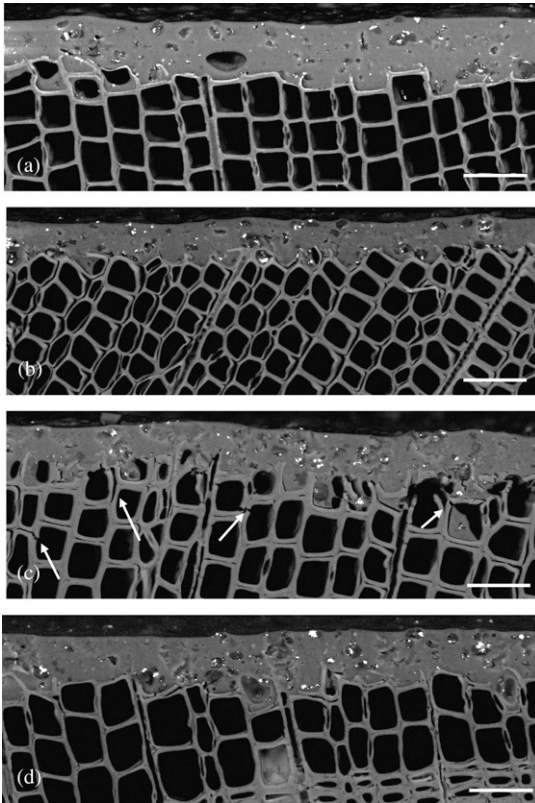


Figure 1. Transverse environmental scanning electron microscopy micrographs of black spruce wood surfaces machined by oblique cutting at an oblique angle of 10° (a), 35° (b), and 60° (c–d). Arrows show microruptures induced in latewood surfaced with an oblique angle of 60° (scale bars = 50  $\mu\text{m}$ ).

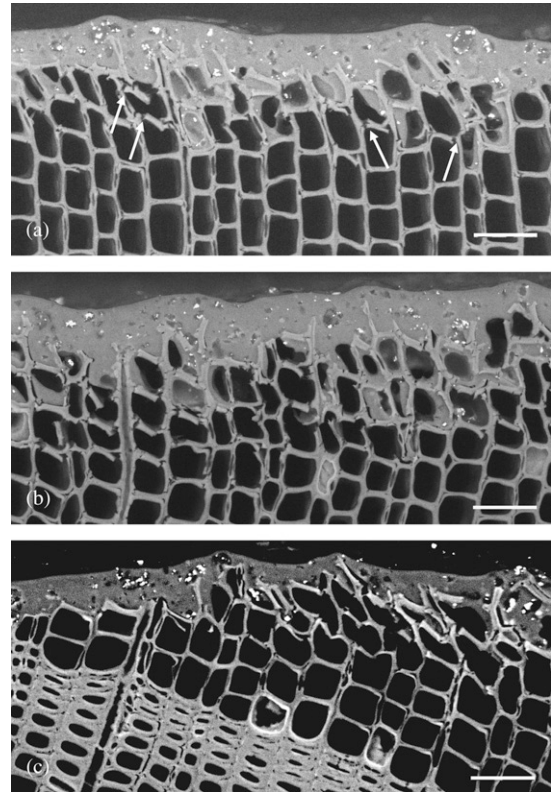


Figure 2. Transverse environmental scanning electron microscopy micrographs of black spruce earlywood machined by face milling at feed per tooth of 0.53 mm (a), 0.34 mm (b), and 0.26 mm (c). Arrows show microruptures induced in face-milled earlywood (scale bars = 50  $\mu\text{m}$ ).

and microruptures were located in the cell walls and in the middle lamella (Fig 3a). At 0.34-mm FT, earlywood suffered extensive damage in the form of cell wall deformation and several microruptures (Fig 2b). The damage extended down the first three to four cells ( $\approx 130 \mu\text{m}$ ). In certain areas, damage in latewood consisted of slight cell crushing and microruptures in the middle lamella and cell walls (Fig 3b). At 0.26-mm FT, the level of subsurface damage for earlywood was similar to that of samples with 0.53-mm FT (Fig 2c). Cells were deformed and crushed down the first two layers ( $\approx 70 \mu\text{m}$ ). Samples were also characterized by microruptures produced by cell wall deformation. Singh et al (2010) explained the effect of

a thin layer of latewood overlying earlywood on raised grain. A similar effect could take place when an earlywood layer overlays latewood, resulting in a greater amount of subsurface damage (Fig 2c). The thinner earlywood cell walls tend to absorb more energy than the more resistant latewood cells. In latewood, the first two layers were crushed and microruptures were observed in the middle lamella and cell walls. Furthermore, coating penetration level differed for earlywood and latewood cells. In earlywood, coating penetration depended on the extent of cell wall deformation and often reached the first two to three cells (Fig 2). In latewood, coating was deposited on surfaces and did not penetrate into samples (Fig 3).

Characteristics of helical-planed surfaces were very similar to those of oblique-cut specimens (Figs 1 and 4). No subsurface damage, such as cell crushing or deformation and microruptures, was observed in the samples (Fig 4). Furthermore, there was no difference between earlywood and latewood areas. Hence, helical planing created surfaces similar to those produced by oblique cutting with an oblique angle less than or equal to  $35^\circ$ . In earlywood, coating penetration often reached the first two cells (Fig 4a). In latewood, coating penetration was similar to that observed for oblique-cut samples

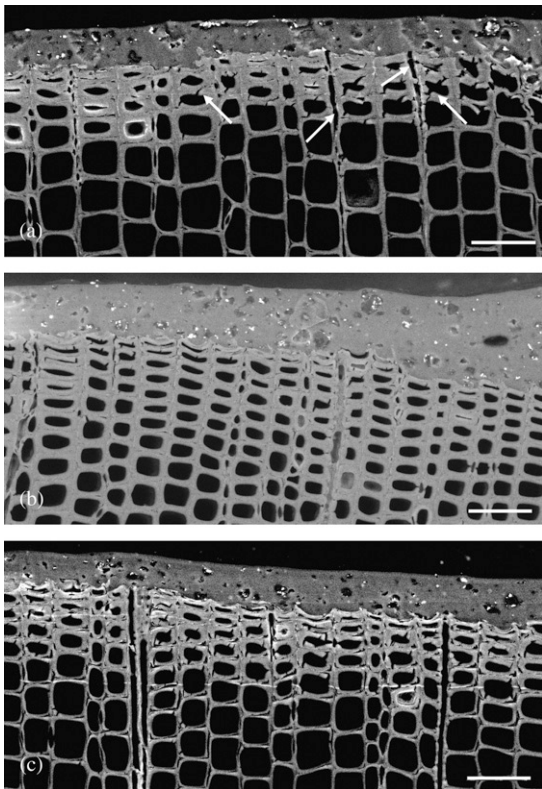


Figure 3. Transverse environmental scanning electron microscopy micrographs of black spruce latewood machined by face milling at feed per tooth of 0.53 mm (a), 0.34 mm (b), and 0.26 mm (c). Arrows show microruptures induced in face-milled latewood (scale bars =  $50 \mu\text{m}$ ).

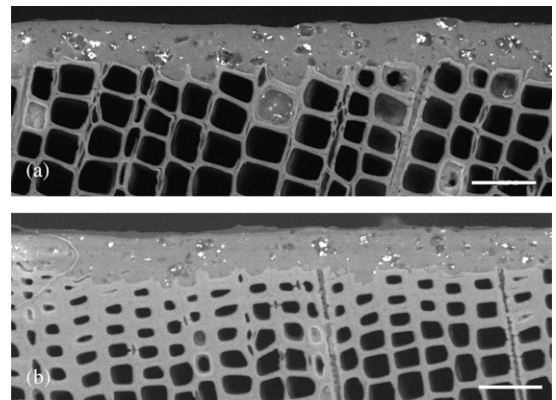


Figure 4. Transverse environmental scanning electron microscopy micrographs of earlywood (a) and latewood (b) black spruce machined by the helical planing process (scale bars =  $50 \mu\text{m}$ ).

(Fig 4b). Hence, the water-borne coating was mainly deposited on the surface and only penetrated the first layer of cells.

**Tangential surfaces.** For the oblique-cut samples, fibrillation level, characterized by partial detachment of tracheids and little crushing, was low but seemed to increase with oblique angle (Fig 5). As shown in Fig 1, the knife edge tended to peel cells apart in or close to the middle lamella. The resulting tangential surfaces appeared smooth with few open lumens, although increasing the oblique angle appeared to increase the number of lumen cells available (Fig 5). Cool and Hernández (2011a), when gluing oblique-cut samples of black spruce, reported that the low number of open lumens decreased adhesive penetration.

Face-milled tangential surfaces were characterized by the highest level of fibrillation of the three studied surfacing processes (Fig 6). As reported by Cool and Hernández (2011a), it was also possible to detect two levels of fibrillation. In certain areas, cells were torn and fibrillation corresponded to portions of cell walls. The thinner cell walls in earlywood were easily torn from the surface (Fig 6a). Conversely, latewood areas had less fibrillation and fibrils appeared to be better attached to the surface, resembling what was reported for sugar maple and paper birch woods (Hernández and Cool 2008a, 2008b; de Moura et al 2010) (Fig 6b). Surface fibrillation could favor mechanical adhesion by enhancing the actual surface available for mechanical anchorage. However, earlywood areas, characterized by torn fibrils, could decrease long-term adhesion of a coating. Furthermore, most lumens were exposed. This contributed to the higher coating penetration observed for earlywood in Fig 2.

Surfaces prepared by helical planing (Fig 7) resembled those surfaced by oblique cutting (Fig 5). Fibrillation was low, whereas helical-planed surfaces had more open lumens than

oblique-cut surfaces. This explains why coating penetrated more in helical-planed surfaces than oblique-cut surfaces.

### Surface Roughness

Torn grain was observed around the knots on oblique-cut surfaces. This defect was attributed to grain deviation close to the knots (Franz 1958; Hernández et al 2001). The incidence of torn grain increased with oblique angle of 60°. The combination of higher lateral cutting force and grain deviation increased the production of this defect. Torn grain was also noted near the knots of surfaces prepared by helical planing. An increase in feed speed resulted in more torn grain as well as deeper defects. Hernández et al (2001) reported that increasing feed speed had a significant impact on maximum depth of defects near or away from white spruce wood knots. Face-milled surfaces did not present any typical surface defects but appeared rougher compared with those that were machined by oblique cutting and helical planing. In orthogonal cutting across the grain with low rake angle, a type III chip was observed by Stewart (1979) regardless of cutting depth. As a result, the relatively low rake angle of 20° used in this study could produce type III chips, which is often associated with higher surface roughness. Moreover, the three FT were shorter than the average length of a tracheid cell (3.6 mm according to Panshin and de Zeeuw [1980]). This indicated that all face-milled surfaces had similar topographies.

For oblique-cut and face-milled samples, cutting parameters had no significant effect on surface roughness parameters (Table 1). In contrast, in helical planing, feed speed had a significant effect on roughness parameters. Oblique-cut samples as well as helical-planed ones prepared at lower feed speeds had the lowest mean surface roughness ( $S_A$  and  $S_Q$ ) (Table 1). Such surfaces were characterized by plateau-like regions, generated by the peeling action of the knife in or close to the middle lamella. When helical planing was performed

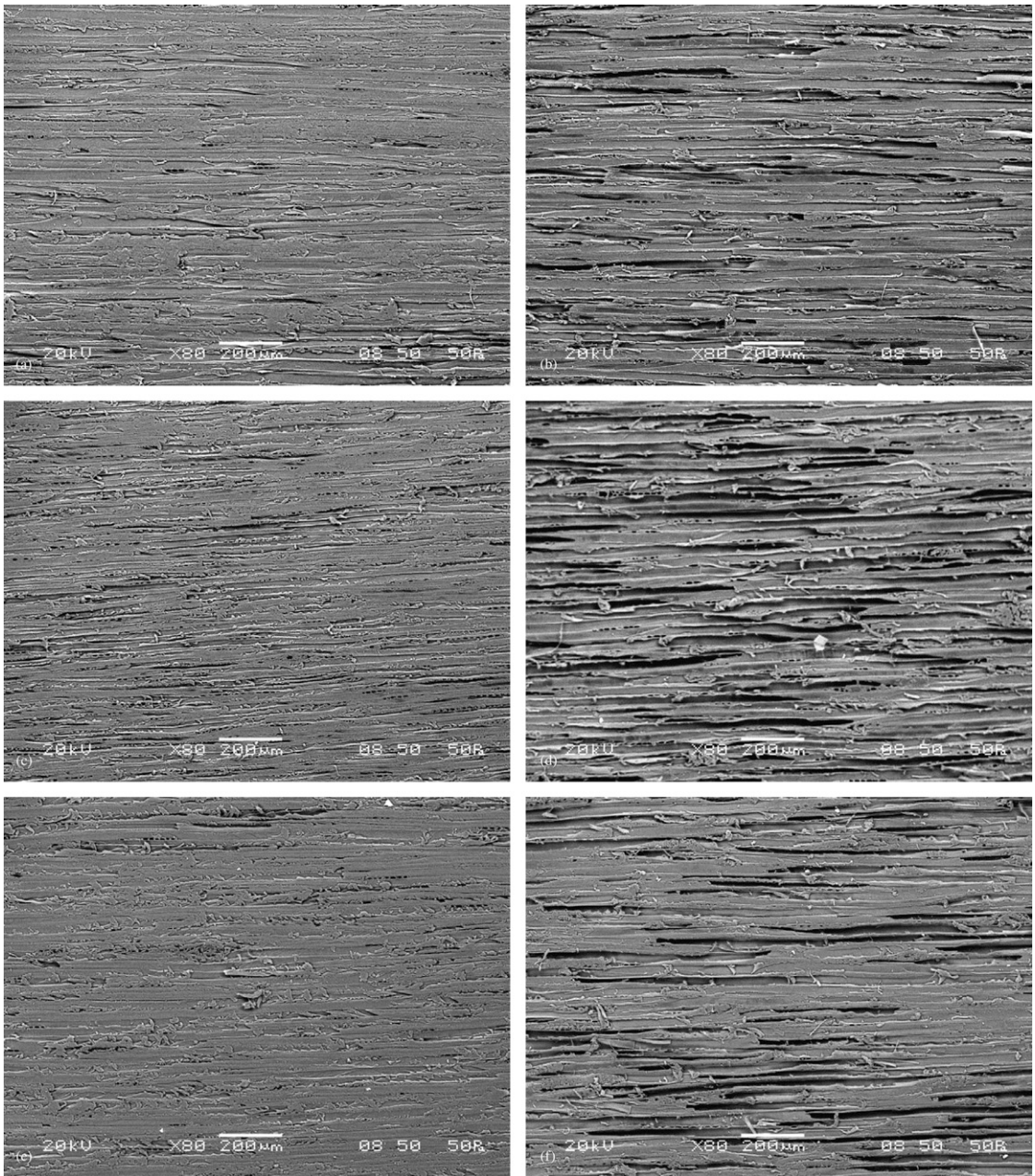


Figure 5. Tangential environmental scanning electron microscopy micrographs of black spruce wood surfaces machined by oblique cutting at oblique angle of 10° (a–b), 35° (c–d), and 60° (e–f).

at a higher feed speed (2.00-mm wavelength), more lumens were exposed. This significantly increased mean surface roughness compared with lower feed speeds. Conversely, the high

fibrillation level combined with the number of open lumens significantly enhanced surface roughness of face-milled samples. Consequently, mean surface roughness parameters

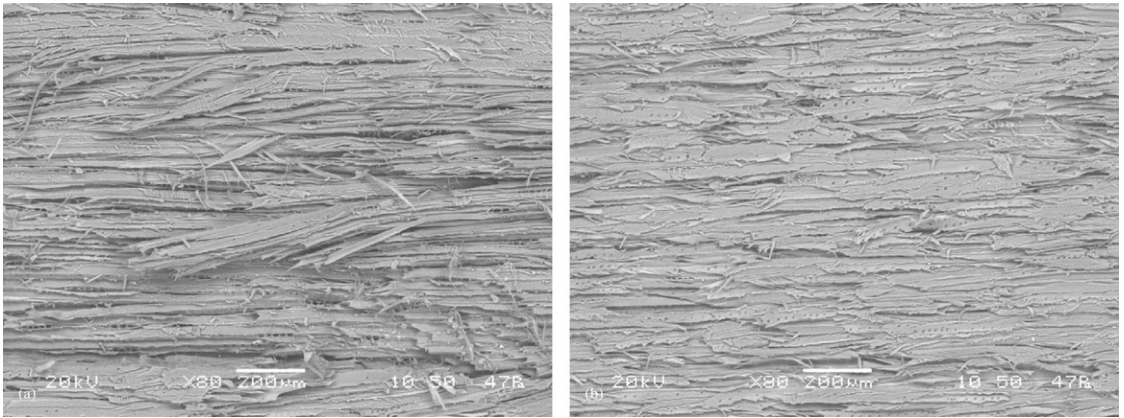


Figure 6. Tangential environmental scanning electron microscopy micrographs of black spruce wood machined by the face milling process.

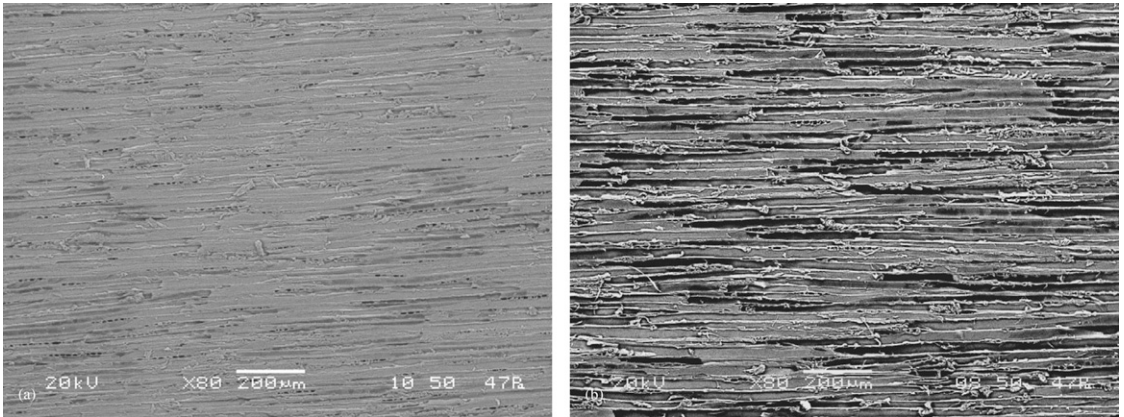


Figure 7. Tangential environmental scanning electron microscopy micrographs of black spruce wood machined by the helical planing process.

were almost two times higher than those of oblique-cut and helical-planed specimens.

Maximum profiles of peak height ( $S_P$ ) and valley depth ( $S_V$ ) behaved similarly to  $S_A$  and  $S_Q$ . As for the latter parameters,  $S_P$  and  $S_V$  were smaller for the oblique-cut and helical-planed surfaces prepared with feed speeds inducing 1.43- and 1.11-mm wavelengths. Increasing feed speed at 2.00-mm wavelength in helical planing resulted in a higher number of open lumens. This agrees with visual observations that revealed an increase in torn grain with feed speed. Hence,  $S_P$  and  $S_V$  were higher for helical

planing at 2.00-mm wavelength. Table 1 also illustrates that both parameters were similar in magnitude for samples prepared by oblique cutting and helical planing. In contrast,  $S_P$  was lower than  $S_V$  for face-milled specimens. Hence, these surfaces were less uniform than the other two. As shown in Fig 6, fibrillation and number of open lumens are both important in face-milled surfaces. Increase in fibrillation level raised the mean line of the profile, which resulted in a higher  $S_V$  parameter (Table 1).

The reduced peak height parameter ( $S_{PK}$ ) has been related to the presence of fuzzy grain

Table 1. 3D surface roughness parameters ( $\mu\text{m}$ ) of black spruce wood specimens prepared by three different planing processes.

Oblique cutting	Oblique angle	$S_A$	$S_Q$	$S_P$	$S_V$	$S_{PK}$	$S_{VK}$						
Oblique cutting	10°	5.5 <sup>a</sup> (0.2) <sup>b</sup>	A <sup>c</sup>	7.3 (0.3)	A	26.9 (1.0)	A	29.4 (1.3)	AB	7.6 (0.3)	AB	9.4 (0.4)	AB
	35°	5.7 (0.3)	A	7.4 (0.4)	A	27.8 (1.2)	A	29.1 (1.6)	A	8.2 (0.4)	ABC	9.1 (0.5)	A
	60°	5.5 (0.2)	A	7.2 (0.3)	A	28.3 (1.0)	A	32.4 (1.2)	BC	7.1 (0.3)	A	9.8 (0.4)	AB
Face milling	Feed per tooth (mm)												
	0.53	10.2 (0.6)	C	13.9 (0.9)	C	41.6 (2.3)	C	65.5 (4.4)	D	10.3 (0.5)	E	21.5 (1.6)	C
	0.34	10.9 (0.8)	C	15.2 (1.0)	C	41.6 (2.5)	C	77.1 (5.5)	D	9.7 (0.5)	DE	25.0 (1.8)	CD
	0.26	11.3 (0.6)	C	15.8 (0.9)	C	46.9 (4.2)	C	80.6 (5.1)	D	10.8 (0.8)	DE	26.3 (1.7)	D
Helical planing	Wavelength (mm)												
	2.00	6.8 (0.2)	B	8.8 (0.3)	B	33.2 (1.0)	B	34.8 (1.5)	C	9.1 (0.4)	CD	10.2 (0.4)	B
	1.43	5.9 (0.2)	A	7.8 (0.3)	A	28.6 (1.0)	A	31.2 (1.3)	ABC	7.7 (0.4)	AB	9.8 (0.5)	AB
	1.11	6.0 (0.2)	A	7.8 (0.2)	A	29.6 (0.9)	AB	29.5 (1.3)	AB	8.8 (0.4)	BCD	8.6 (0.4)	A

<sup>a</sup> Mean of 30 replicates.

<sup>b</sup> Standard error of mean in parentheses.

<sup>c</sup> Means within a column followed by the same letter are not significantly different at the 5% probability level.

(Fujiwara et al 2005; Gurau et al 2005). Because this surface defect was not observed on the surfaces,  $S_{PK}$  could be related to fibrillation level. Oblique-cut samples had the lowest  $S_{PK}$  values probably because of low fibrillation on their surfaces (Table 1).  $S_{PK}$  was higher for the helical-planned surfaces, which also showed a low fibrillation but more open lumens. Such lumens lowered the mean line of the profile, thus increasing  $S_{PK}$  value. In contrast, face-milled specimens clearly had a higher fibrillation level than that observed on the other samples. Thus, these surfaces were associated with high values of  $S_{PK}$ .

Reduced valley depth ( $S_{VK}$ ) followed the same pattern as the other surface roughness parameters.  $S_{VK}$  is in fact related to the number of open lumens (Fujiwara et al 2005). As seen in Figs 5 and 7, oblique-cut and helical-planned samples were characterized by similar anatomic features. Hence,  $S_{VK}$  was similar for these two surfaces (Table 1). However, face-milled surfaces had

much more open lumens, which resulted in higher values of  $S_{VK}$ . For face-milled samples, Table 1 also shows that  $S_{VK}$  was higher than  $S_{PK}$ . The high fibrillation level on these surfaces raised the mean line of the surface roughness profile, which increased  $S_{VK}$  to the detriment of  $S_{PK}$ . As for  $S_P$  and  $S_V$ , similar  $S_{VK}$  and  $S_{PK}$  were associated with uniform tangential surfaces.

## Wettability

The progression of the contact angle of a pure water drop is illustrated in Fig 8 for all studied cutting conditions. It clearly shows that different planing processes and cutting parameters affected the wetting properties of black spruce wood surfaces. Gindl et al (2001) reported similar results for four wood species that were sanded or microtomed. Oblique-cut surfaces were significantly affected by oblique angle. Surfaces were significantly more hydrophilic when oblique angle of 60° was used.

The disperse component of the surface energy increased significantly when this angle was used (Table 2). Thus, more sites could be available for hydrogen linkages between the wood surface and the water-borne coating. For face-milled samples, FT had a significant effect on the wetting properties (Fig 8), although fibrillation and amount of open lumens were similar for the three studied FT. A higher

FT (0.53 mm) also appeared to induce surfaces with a significantly higher polar surface energy component (Table 2). The progression of contact angle on the helical-planed surfaces was significantly affected by feed speed (Fig 8). However, there seemed to be a second-order effect because surfaces prepared with the intermediate feed speed showed better wetting properties. Nevertheless, these observations were not confirmed when data of surface energy were calculated (Table 2). In this case, as feed speed increased, disperse component decreased, polar component increased, and total surface energy remained unchanged.

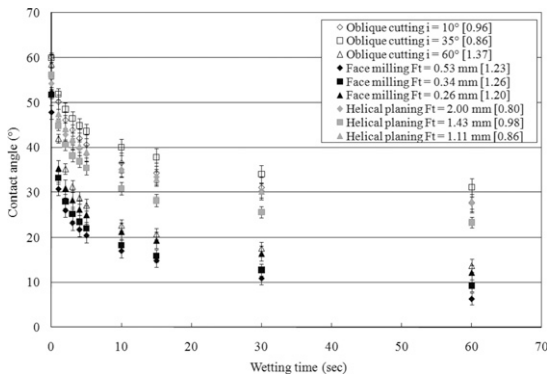


Figure 8. Progression of the contact angle for the three studied planing processes. For every cutting parameter, mean value of the wetting rate is in brackets.

### Adhesion Tests

Before the aging treatment, pull-off strength was statistically similar for samples prepared by the three planing processes (Table 3). After accelerated aging treatment, face-milled surfaces showed significantly lower pull-off strength. After this aging, oblique-cut surfaces as well as those prepared by helical planing at 2.00- and 1.43-mm wavelengths had significantly higher

Table 2. Surface energy components ( $\text{mJ}/\text{m}^2$ ) determined by the harmonic mean method for black spruce wood specimens prepared by three different planing processes.

Oblique cutting	Oblique angle	Disperse		Polar		Total	
	10°	16.5 <sup>a</sup> (0.6) <sup>b</sup>	A <sup>c</sup>	27.8 (0.9)	AB	44.3 (0.7)	A
	35°	16.3 (0.6)	A	28.0 (0.9)	AB	44.3 (0.6)	A
	60°	19.3 (0.4)	BC	26.5 (0.6)	A	45.8 (0.5)	B
Face milling	Feed per tooth (mm)						
	0.53	20.6 (0.4)	DE	32.4 (1.1)	C	53.0 (0.9)	E
	0.34	21.0 (0.3)	E	29.6 (0.7)	B	50.6 (0.5)	D
	0.26	21.7 (0.5)	E	29.0 (0.9)	B	50.7 (0.6)	D
Helical planing	Wavelength (mm)						
	2.00	18.8 (0.4)	B	29.7 (0.9)	BC	48.5 (0.7)	C
	1.43	18.7 (0.3)	B	28.3 (0.6)	B	47.1 (0.4)	C
	1.11	20.0 (0.2)	CD	27.7 (0.5)	AB	47.7 (0.4)	C

<sup>a</sup> Mean of 30 replicates.

<sup>b</sup> Standard error of mean in parentheses.

<sup>c</sup> Means within a column followed by the same letter are not significantly different at the 5% probability level.

Table 3. Pull-off strength (MPa) before and after an accelerated aging treatment for black spruce wood specimens prepared by three different planing processes.

Oblique cutting	Oblique angle	Before aging		After aging		Adhesion loss (%)	
	10°	4.1 <sup>a</sup> (0.1) <sup>b</sup>	A <sup>c</sup>	3.2 (0.1)	AB	22	ABC
	35°	3.9 (0.2)	A	3.3 (0.2)	A	15	A
	60°	4.2 (0.1)	A	3.5 (0.1)	A	17	AB
Face milling	Feed per tooth (mm)						
	0.53	3.8 (0.1)	A	2.7 (0.1)	D	29	BC
	0.34	4.0 (0.2)	A	2.7 (0.1)	D	33	C
	0.26	3.9 (0.1)	A	2.8 (0.1)	BCD	28	BC
Helical planing	Wavelength (mm)						
	2.00	4.1 (0.2)	A	3.1 (0.1)	ABC	24	AB
	1.43	4.3 (0.2)	A	3.3 (0.2)	A	23	AB
	1.11	3.9 (0.2)	A	2.8 (0.1)	CD	28	BC

<sup>a</sup> Mean of 30 replicates.

<sup>b</sup> Standard error of mean in parentheses.

<sup>c</sup> Means within a column followed by the same letter are not significantly different at the 5% probability level.

pull-off strengths (Table 3). Measured adhesion was similar to that reported for sanded black spruce wood coated with the same water-borne varnish (Cool and Hernández 2011b). Furthermore, these oblique-cut and helical-planed samples were among those that underwent the lowest adhesion loss during aging. Although it was not significant, oblique-cut samples planed with an oblique angle of 35 and 60° lost less of their initial adhesion. Consequently, this surfacing process could be interesting for long-term purposes. The absence of subsurface damage as well as the slight fibrillation appeared to favor mechanical adhesion in open lumens and to decrease the effect of weathering treatment. The opposite was observed when oblique-cut black spruce wood samples were glued (Cool and Hernández 2011a). As previously mentioned, absence of fibrillation could have favored squeeze-out of glue, resulting in starved glue joints and lower resistance to weathering. Because the oblique angle of 35° induced less torn grain than that of the 60°, which underwent a similar adhesion loss, the former is recommended. In the case of helical planing, a

wavelength of 1.43 mm appears suitable because less torn grain was generated.

Face-milled samples had the lowest pull-off strength after aging and suffered the greatest loss in adhesion. They also showed the highest level of fibrillation, coating penetration, and subsurface damage. Although fibrillation and coating penetration could increase mechanical adhesion, numerous microruptures were probably generated during the moisturizing–drying cycles. Thus, adhesion at the wood-coating interface was decreased. The opposite was observed when gluing face-milled black spruce surfaces (Cool and Hernández 2011a). In that case, surface characteristics favored glue penetration while decreasing squeeze-out of glue. This combination generated a high-quality glue joint with good resistance to accelerated weathering. The fact that glued surfaces are not directly exposed to weather probably changes the quality requirements. Also, rougher surfaces need higher spreading rates to perform adequately (Richter et al 1995). In this study, the same spreading rates were applied on all

surfaces to reflect typical procedures used in the industry. Based on the results obtained by Richter et al (1995), it can be assumed that pull-off strength would improve and production costs would increase if higher spreading rates were used on face-milled surfaces. Increasing rake angle could also help to decrease surface roughness and improve pull-off strength.

No correlations were obtained between surface quality parameters and pull-off strength. Similar results were obtained by Cool and Hernández (2011b) with coated samples of sanded black spruce wood. Consequently, pull-off strength has to be determined to measure coating performance on black spruce wood.

### CONCLUSIONS

Oblique-cut and helical-planed surfaces had similar features. These samples had low subsurface damage as well as little fibrillation. In addition, some cell lumens were accessible on the surface, which favored coating penetration. This resulted in samples having lower surface roughness and wetting properties compared with face-milled samples. The latter were defined by more subsurface damage, higher fibrillation, and a higher number of available lumens, which resulted in deeper coating penetration. However, pull-off strength of face-milled samples was significantly lower after weathering compared with those that were oblique-cut or helical-planed. Consequently, oblique cutting or helical planing are both recommended as surfacing processes prior to coating application because pull-off strength was similar to that of sanded samples. No correlations were obtained between surface quality parameters and pull-off tests, which indicates that the latter are required in quantifying coating performance of black spruce surfaces. Considering that this research was done with freshly sharpened knives, future research should take into account the wear phenomena of cutting tools. Such a study would give information on sharpening frequency, which affects production costs. Future research should also take into account spreading rate and rake angle and how these variables could

improve pull-off strength of face-milled samples after weathering. Combined with a study on production costs, this would further facilitate selection of the best machining process.

### REFERENCES

- ASTM (1998) D 3459. Standard test method for humidity cycling for coatings on wood and wood products. American Society for Testing and Materials, West Conshohocken, PA.
- ASTM (2002) D 4541. Standard test method for pull-off strength of coatings using portable adhesion testers. American Society for Testing and Materials, West Conshohocken, PA.
- Cool J, Hernández RE (2011a) Evaluation of four surfacing methods on black spruce wood in relation to poly (vinyl acetate) gluing performance. *Wood Fiber Sci* 43(2):194-205.
- Cool J, Hernández RE (2011b) Improving the sanding process of black spruce wood for surface quality and water-based coating adhesion. *Forest Prod J* (in press).
- de Meijer M, Haemers S, Cobben W, Militz H (2000) Surface energy determinations of wood: Comparison of methods and wood species. *Langmuir* 16(24):9352-9359.
- de Meijer M, Thurich K, Militz H (1998) Comparative study on penetration characteristics of modern wood coatings. *Wood Sci Technol* 32(5):347-365.
- de Moura LF, Cool J, Hernández RE (2010) Anatomical evaluation of wood surfaces produced by oblique cutting and face milling. *IAWA J* 31(1):77-88.
- de Moura LF, Hernández RE (2005) Evaluation of varnish coating performance for two surfacing methods on sugar maple wood. *Wood Fiber Sci* 37(2):355-366.
- de Moura LF, Hernández RE (2006a) Effects of abrasive mineral, grit size and feed speed on the quality of sanded surfaces of sugar maple wood. *Wood Sci Technol* 40(6):517-530.
- de Moura LF, Hernández RE (2006b) Evaluation of varnish coating performance for three surfacing methods on sugar maple wood. *Forest Prod J* 56(11/12):130-136.
- de Moura LF, Hernández RE (2007) Characteristics of sugar maple wood surfaces machined with the fixed-oblique-knife pressure-bar cutting system. *Wood Sci Technol* 41(1):17-29.
- d'Errico A, Pasian S, Baratti A, Zanelli R, Alfonso S, Gilardi L, Beatrice F, Bena A, Costa G (2009) A case-control study on occupational risk factors for sino-nasal cancer. *Occup Environ Med* 66(7):448-455.
- Franz NC (1958) An analysis of the wood-cutting process. University of Michigan Press, Ann Arbor, MI. 152 pp.
- Fujiwara Y, Fujii Y, Okumura S (2005) Relationship between roughness parameters based on material ratio curve and tactile roughness for sanded surfaces of two hardwoods. *J Wood Sci* 51(3):274-277.

- Gardner DJ, Generalla NC, Gunnells DW, Wolcott MP (1991) Dynamic wettability of wood. *Langmuir* 7(11):2498-2502.
- Gindl M, Sinn G, Reiterer A, Tschegg S (2001) Wood surface energy and time dependence of wettability: A comparison of different wood surfaces using an acid-base approach. *Holzforschung* 55(4):433-440.
- Gurau L, Mansfield-Williams H, Irle M (2005) Processing roughness of sanded wood surfaces. *Holz Roh Werkst* 63(1):43-52.
- Hall A, Heard J (1982) *Wood finishing and refinishing*. Holt, Rinehart and Winston, New York, NY. 196 pp.
- Hernández RE, Bustos C, Fortin Y, Beaulieu J (2001) Wood machining properties of white spruce from plantation forests. *Forest Prod J* 51(6):82-88.
- Hernández RE, Cool J (2008a) Effects of cutting parameters on surface quality of paper birch wood machined across the grain with two planing techniques. *Holz Roh Werkst* 66(2):147-154.
- Hernández RE, Cool J (2008b) Evaluation of three surfacing methods on paper birch wood in relation to water- and solvent-borne coating performance. *Wood Fiber Sci* 40(3):459-469.
- ISO (1996) 13565-2. Geometrical product specifications (GPS). Surface texture. Profile method; Surfaces having stratified functional properties. Part 2: Height characterisation using the linear material ratio curve. International Standards Organization. British Standards Institute, London, UK.
- ISO (1997) 4287. Geometrical product specifications (GPS). Surface texture. Profile Method. Terms. Definitions and surface Texture parameters. International Standards Organization. British Standards Institute, London, UK.
- ISO (2002) 16610-31. Geometrical product specifications (GPS)—Filtration part 31: Robust profile filters. Gaussian regression filters. In draft. International Standards Organization. British Standards Institute, London, UK.
- Jin W, Cai L (1996) Study and analysis on cutting forces of oblique cutting of wood. *Holz Roh Werkst* 54(4):283-286.
- Jin W, Cai L (1997) Study on the normal component force in oblique cutting of wood. *Holz Roh Werkst* 55(2):118-120.
- Jones CW (1994) *Cutterheads and knives for machining wood*. C.W. Jones, Seattle, WA. 138 pp.
- Koch P (1976) Prototype flaking head smooths surfaces left by headrig or edger chipping heads. *Forest Prod J* 26(12):22-27.
- Murmanis L, River BH, Stewart H (1983) Microscopy of abrasive-planed and knife-planed surfaces in wood-adhesive bonds. *Wood Fiber Sci* 15(2):102-115.
- Murmanis L, River BH, Stewart HA (1986) Surface and subsurface characteristics related to abrasive-planing conditions. *Wood Fiber Sci* 18(1):107-117.
- Ozaki S, Kimura S (1989) The oblique cutting of wood. V. Splits below the cutting plane and the ratio of shrinkage of the chips in a 90°-90° cutting situation. *Mokuzai Gakkaishi* 35(1):896-904.
- Panshin AJ, de Zeeuw C (1980) *Textbook of wood technology*. McGraw-Hill, New York, NY. 722 pp.
- Piao C, Winandy JE, Shupe TF (2010) From hydrophilicity to hydrophobicity: A critical review: Part 1. Wettability and surface behavior. *Wood Fiber Sci* 42(4):490-510.
- Richter K, Feist WC, Knaebe MT (1995) The effect of surface roughness on the performance of finishes. Part 1. Roughness characterization and stain performance. *Forest Prod J* 45(7/8):91-97.
- SAS (2007) *SAS/STAT users' guide, version 9.2*. Statistical Analysis Software Institute Inc., Cary, NC.
- Singh AP, Dawson BSW, Hands KD, Ward JV, Greaves M, Turner JCP, Rickard CL (2010) The anatomy of raised grain on pinus radiata weatherboards. *IAWA J* 31(1):67-76.
- Stewart HA (1971) Chips produced with a helical cutter. *Forest Prod J* 21(5):44-45.
- Stewart HA (1974) Face milling can improve for surfacing and flaking. *Forest Prod J* 24(2):58-59.
- Stewart HA (1979) Analysis of orthogonal woodcutting across the grain. *Wood Sci* 12(1):38-45.
- Stewart HA (1980) Some surfacing defects and problems related to wood moisture content. *Wood Fiber Sci* 12(3):175-182.
- Stewart HA (1989) Fixed-knife pressure-bar planing method reduces or eliminates subsurface damage. *Forest Prod J* 39(7/8):66-70.
- Stewart HA, Crist JB (1982) SEM examination of subsurface damage of wood after abrasive and knife planing. *Wood Sci* 14(3):106-109.
- Stewart HA, Lehmann WF (1974) Cross-grain cutting with segmented helical cutters produces good surfaces and flakes. *Forest Prod J* 24(9):104-106.
- Stewart JS (1975) Noise-reducing tooling for planer noise control. Pages 174-187 in *Modern Sawmill Techniques*. Vol. 4. Proc 4th Sawmill Clinic, New Orleans, LA, November 1974. HG Lambert, ed. Miller Freeman Publications, San Francisco, CA.
- Stewart JS, Hart FD (1976) Control of industrial wood planer noise through improved cutterhead design. *Noise Control Eng* 7(1):4-9.
- Taylor JB, Carrano AL, Lemaster RL (1999) Quantification of process parameters in a wood sanding operation. *Forest Prod J* 49(5):41-46.
- Wang S, Zhang Y, Xing C (2007) Effect of drying method on the surface wettability of wood strands. *Holz Roh Werkst* 65:437-442.
- Wolkenhauer A, Avramidis G, Cai Y, Militz H, Viöl W (2007) Investigation of wood and timber surface modification by dielectric barrier discharge at atmospheric pressure. *Plasma Process Polym* 4(1):S470-S474.
- Wu S (1971) Calculation of interfacial tension in polymer systems. *J Polym Sci Pol Lett* 34:19-30.